Ecological Applications, 30(5), 2020, e02101

Solar-induced chlorophyll fluorescence and short-term photosynthetic response to drought

Levi T. Helm [1,2] Hanyu Shi [2] Manuel T. Lerdau [2] and Xi Yang [2,3]

[1]*School of Life Sciences, Arizona State University, 427 East Tyler Mall, Tempe, Arizona 85281 USA*
[2]*Department of Environmental Sciences, University of Virginia, 291 McCormick Road, Charlottesville, Virginia 22904 USA*

Citation: Helm, L. T., H. Shi, M. T. Lerdau, and X. Yang. 2020. Solar-induced chlorophyll fluorescence and short-term photosynthetic response to drought. Ecological Applications 30(5):e02101. 10.1002/eap.2101

Abstract. Drought is among the most damaging climate extremes, potentially causing significant decline in ecosystem functioning and services at the regional to global scale, thus monitoring of drought events is critically important. Solar-induced chlorophyll fluorescence (SIF) has been found to strongly correlate with gross primary production on the global scale. Recent advances in the remote sensing of SIF allow for large-scale, real-time estimation of photosynthesis using this relationship. However, several studies have used SIF to quantify the impact of drought with mixed results, and the leaf-level mechanisms linking SIF and photosynthesis are unclear, particularly how the relationship may change under drought. We conducted a drought experiment with 2-yr old *Populus deltoides*. We measured leaf-level gas exchange, SIF, and pulse amplitude modulated (PAM) fluorescence before and during the 1-month drought. We found clear responses of net photosynthesis and stomatal conductance to water stress, however, SIF showed a smaller response to drought. Net photosynthesis (A_{net}) and conductance dropped 94% and 95% on average over the drought, while SIF values only decreased slightly (21%). Electron transport rate dropped 64% when compared to the control over the last week of drought, but the electron transport chain did not completely shut down as A_{net} approached zero. Additionally, SIF yield (SIF_y) was positively correlated with steady-state fluorescence (F_s) and negatively correlated with non-photochemical quenching (NPQ; $R^2 = 0.77$). Both F_s and SIF_y, after normalization by the minimum fluorescence from a dark-adapted sample (F_o), showed a more pronounced drought response, although the results suggest the response is complicated by several factors. Leaf-level experiments can elucidate mechanisms behind large-scale remote sensing observations of ecosystem functioning. The value of SIF as an accurate estimator of photosynthesis may decrease during mild stress events of short duration, especially when the response is primarily stomatal and not fully coupled with the light reactions of photosynthesis. We discuss potential factors affecting the weak SIF response to drought, including upregulation of NPQ, change in internal leaf structure and chlorophyll concentration, and photorespiration. The results suggest that SIF is mainly controlled by the light reactions of photosynthesis, which operate on different timescales than the stomatal response.

Key words: *chlorophyll fluorescence; drought; photosynthesis; remote sensing; solar-induced chlorophyll fluorescence; stomatal conductance.*

Introduction

Photosynthetic carbon uptake is one of the largest carbon dioxide fluxes on Earth's surface and measuring photosynthesis on a global scale is essential for understanding the Earth's carbon budget (Beer et al. 2010, Berry et al. 2013, Ryu et al. 2019). The state-of-art methods, however, contain significant uncertainties in capturing the spatiotemporal patterns of global gross primary production (GPP; Schaefer et al. 2012, Verma et al. 2014). Recent advances in the remote sensing of solar-induced chlorophyll fluorescence (SIF) allow for large-scale, real-time, physiologically derived estimations of photosynthetic carbon uptake. These estimations utilize the relationship between SIF and electron transport during the light reactions of photosynthesis and the mechanistic connections between electron transport and carbon fixation and reduction during the dark reactions of photosynthesis (Meroni et al. 2009, Frankenberg et al. 2011, Joiner et al. 2011, Yang et al. 2015, 2017, 2018, Miao et al. 2018, Magney et al. 2019, Mohammed et al. 2019). However, most of the research linking SIF and GPP is based on larger-scale relationships correlating SIF and GPP estimates from models or eddy covariance towers (Parazoo et al. 2014, Sun et al. 2017). Leaf-level measurements and experiments are needed to understand the fundamental mechanisms linking SIF

Manuscript received 11 October 2019; revised 30 December 2019; accepted 24 January 2020. Corresponding Editor: David S. Schimel.
[3] Corresponding Author. E-mail: xiyang@virginia.edu

and photosynthesis, especially under stress such as drought, so that the effects of these stressors on the relationships can be used to estimate ecosystem function with large-scale SIF data.

The impacts of environmental factors such as water availability on the relationship between SIF and carbon uptake are not well understood. In a changing climate where ecosystems experience more frequent stress (e.g., droughts), variations in the SIF–photosynthesis relationship potentially add substantial uncertainty to large-scale carbon exchange estimates (Porcar-Castell et al. 2014, Cendrero-Mateo et al. 2015). The response of the light reactions and dark reactions of photosynthesis may operate on different time scales, a faster stomatal response to drought than a response in electron transport may alter the relationship (Gu et al. 2019). Understanding the effects of environmental stress on the SIF-photosynthesis relationship requires simultaneous measurements of these processes under field and controlled conditions to elucidate the mechanistic relationships, which may then be used in Earth system models (Lee et al. 2015, Raczka et al. 2019).

During photosynthesis, the radiation that chlorophyll absorbs (absorbed photosynthetically active radiation or APAR) has several possible fates. This absorbed radiation can be used to produce and transfer protons. It can also dissipate as fluorescence or heat (Demmig-Adams and Adams 2006, Baker 2008). Because these processes, with respect to any absorbed quantum of light, are mutually exclusive, they, in effect, compete with one another (Murchie and Lawson 2013). This competition is captured in Eq. 1, where each term is the proportion of energy dissipated in each pathway respectively. ΦP is the radiation utilized for photochemistry, ΦNPQ is the proportion of energy dissipated through NPQ, ΦF is the proportion of energy dissipated as fluorescence, and ΦD is basal heat dissipation

$$1 = \Phi P + \Phi NPQ + \Phi F + \Phi D. \quad (1)$$

The fluorescence term, when multiplied by the fraction of absorbed light (APAR) and the fluorescence escape factor (ε), which is related to sensor-viewing geometry and canopy structure, yields solar-induced fluorescence (Eq. 2).

$$SIF = APAR*\Phi F*\varepsilon. \quad (2)$$

This fluorescence product can be measured passively by remote sensing at the wavelength(s) of fluorescence. In this experiment, SIF is measured at 760 nm. From the above equations, one can see that SIF is not a direct measurement of photosynthetic productivity but a competing pathway for absorbed energy. SIF yield (SIF_y), which is the ratio between SIF and APAR, is conceptually equivalent to ΦF in Eq. 1. Leaf-level measurements indicate that ΦP decreases while ΦF increases when APAR is low (e.g., low light conditions during the dawn and dusk), and ΦP and ΦF both decrease when APAR is high (Porcar-Castell et al. 2014, van der Tol et al. 2014). Although the above-described relationship is known qualitatively, the quantitative dynamics between SIF and photosynthesis are not well understood, and the sensitivity of these dynamics to environmental factors is only beginning to be examined (van der Tol et al. 2014). The yield of each pathway can be explicitly determined though inhibition of the other pathways (Magney et al. 2017).

The photons that go to photochemistry are utilized for non-cyclic electron transport through photosystem II (PSII), ultimately providing electrons for chloroplast metabolism, including the Calvin cycle. The electron transport rate (ETR) is thus proportional to the efficiency of PSII and the APAR (Genty et al. 1989, Baker 2008). Under normal environmental conditions, there is a strong correlation between net photosynthetic carbon assimilation and electron transport rate, however, under severe water deficit this link weakens (Flexas et al. 1999, Baker 2008).

During water stress, plants close their stomata, often occurring with an increase in NPQ and photorespiration (PR), which is the oxidation of ribulose bisphosphate rather than its carboxylation (Flexas et al. 2002), potentially altering the relationship between SIF and carbon uptake. Studies demonstrate that drought stress causes a decrease in net photosynthesis but has a smaller effect on electron transport rate, likely because photorespiration serves as an alternative sink for electrons (Flexas et al. 1998). Better understanding of the mechanistic bases for SIF, and how they are altered under stress, is essential for using SIF data to estimate carbon exchange on large spatiotemporal scales and across a variety of conditions.

Early leaf-level experiments investigating the relationship between fluorescence and photosynthesis suggested that steady-state fluorescence (F_s), when normalized by steady-state fluorescence under dark-adapted conditions (F_o) is an indicator of CO_2 assimilation under water stress (Flexas et al. 2002). From these results, the remote sensing of steady-state fluorescence was suggested as a tool for detection of plant water stress, although with the acknowledgement that there are complications to the using the measurement as a proxy for drought stress (Flexas et al. 2002).

We report on simultaneous measurements of passively and actively measured leaf fluorescence as well as gas exchange during a short-term drought experiment. We show the temporal dynamics of key gas exchange, biochemical, and fluorescence parameters, and their relationships. These measurements allow insight into the physiological mechanisms connecting SIF and photosynthesis at the leaf level. We present the results as SIF measurements relating to net photosynthesis measurements and also as normalized fluorescence parameters relating to net photosynthesis. The former has implications for measurement of SIF in relation to

photosynthesis during drought stress, and the normalized parameters relate to previous leaf-level fluorescence–photosynthesis experiments under drought stress.

Methods

Experimental design

Eastern cottonwood (*Populus deltoides*), a tree species widely distributed in the United States, was chosen for the study. Bare root stock saplings purchased from Cold Stream Farm in Michigan were grown in the University of Virginia Greenhouse in Charlottesville, Virginia, USA, over the summer starting in late May 2017. Trees were 2-yr-old single-leader saplings that ranged between 1 and 1.5 m. Leaves were fully expanded by 20 July 2017.

Beginning in early September, eight representative trees were chosen for experimentation, and a mature, fully expanded leaf on each was tagged. To control for leaf age variation in metabolism, the leaf plastochron index (LPI), an indication of relative leaf age (Isebrands and Larson 1973), was used to control for leaf development: every several days leaves were retagged to maintain an LPI of approximately 6–8 on the apical shoot. Previous studies of photosynthesis in *P. deltoides* have shown that leaves in this age range are functionally very similar (Funk et al. 1999). Four of the eight trees, chosen at random, were subjected to drought stress and were not watered.

The experiment lasted 28 d. Each measurement day, the experimental trees were taken outside between the hours of 11:00 and 14:00. Three nearly contemporaneous measurements (gas exchange, PAM fluorescence, and SIF) were made on each leaf, all with the leaf oriented horizontally. The leaf was placed horizontally in the leaf chamber while measuring gas exchange, then the same leaf was held by the petiole at the same angle and measured at the same location on the leaf for the final two measurements. First, survey-type gas exchange measurements were made with the LI6800 Portable Photosynthesis system (Li-COR, Lincoln, Nebraska, USA), then pulse amplitude modulated (PAM) fluorimetry was measured using a PAM-2500 (Heinz Walz GmbH, Effeltrich, Germany). Lastly, a portable field spectrometer (QEpro, OceanOptics, Dunelin, Florida, USA) was used to estimate the leaf-level SIF (the following sections describe these three survey-type measurements in detail). The measurement cycle was timed so that changes in solar radiation due to clouds were minimized by starting the cycle during stable PAR. We used the PAR measurement from LI-6800 (Q_{in}, $\mu mol \cdot m^{-2} \cdot s^{-1}$) and the irradiance at 755 nm measured from QEpro to screen measurements when the light condition changed rapidly, and outliers were excluded using the Sidak one-step correction in the Python package statsmodels outlier tests (a total of 22 points were discarded, see Appendix S1: Fig. S7). Generally, less than one minute elapsed between collection of the gas exchange measurement and the final SIF measurement.

Additional measurements

Daily measurements of soil moisture content were made to evaluate drought progression using a Campbell Scientific HydroSense II soil moisture probe (Campbell Scientific, Logan, Utah, USA). Measurements of leaf chlorophyll concentration were taken daily using a SPAD-502 chlorophyll meter (Spectrum Technologies, Aurora, Illinois, USA); the average of three measurements across the leaf was recorded.

Every 4–5 d, several hours before the survey measurements were conducted, dark-adapted leaf fluorescence measurements were made by allowing the leaves to dark adapt with Walz leaf clips for 15 minutes, then performing a dark-adapted light pulse using the PAM-2500 with the default settings and measuring light intensity set to 4, and the saturation pulse intensity set to 10 (the PAM settings are arbitrary numbers. This setting corresponds to a saturation pulse of roughly 8,300 $\mu mol \cdot m^{-2} \cdot s^{-1}$ [Heinz Walz GmbH 2008]). Dark-adapted PAM measurements, which give F_m and F_o of each sample, were not taken daily but at an interval of roughly each week (the experiment continued from DOY 251–279 [day of the year, with 1 January = 1], dark-adapted measurements were taken on DOY 258, 263, 267, 272, and 276). To use dark-adapted measurements, F_o was linearly interpolated between measurement days. At the beginning and end of the experiment, F_o was taken to be the temporally closest measured value as opposed to extrapolating data points.

Gas exchange

Gas exchange measurements were made using the LI6800 system with a 3 × 3 cm clear top chamber. Every day, each of the eight plants was measured once. The chamber was controlled to have a relative humidity of 70% and a CO_2 concentration of 400 ppm. Humidity was maintained at 70% for two reasons. This value was close to the ambient humidity during measurement time, and previous work on *Populus* has demonstrated that stomatal conductance is relatively insensitive to humidity from 60% to 80% (Funk et al. 2004, Funk et al. 2007). Flow rate was adjusted to account for differences in stomatal closure during the drought. Within any one measurement, flow was held constant. The temperature was set to match the ambient outdoor temperature measured using an external thermocouple. The LI-6800 head was placed on top of a tripod and clamped over the leaf such that the leaf filled the entire chamber and the incident light was not shaded by the LI-6800 head. After the system stabilized, a standard survey-type measurement of the gas exchange variables, including net photosynthetic carbon assimilation (A_{net}), was recorded. Stabilization was defined by the coefficient of variation for

water and carbon dioxide flux being <0.5%, the time to stabilize varied from leaf to leaf, but was usually within eight minutes.

Pulse amplitude modulated fluorescence

Active fluorescence measurements were made using a PAM-2500 fluorometer. The fiber was held by the clip at a 60° angle oriented toward the south, and the clip was attached to the leaf at approximately the location the gas exchange measurement was made. The fluorometer settings were set to default, except the measuring light intensity, which was set to 4 for all measurements (arbitrary number). A standard saturation pulse following the procedure described in the lab manual (Heinz Walz GmbH 2008) was conducted in order to record the light-adapted fluorescence properties of the leaf.

Pulse amplitude modulated (PAM) fluorescence analyses operate by stimulating the leaf with high intensity light to saturate the photosystem, thus closing the receptor centers and observing the maximum amount of fluorescence that occurs. Under light-adapted conditions, this maximum fluorescence is termed F'_m. When the leaves are dark-adapted, that is, when PSII is fully open, a saturation pulse will cause the PSII reaction centers to close. The peak level of fluorescence measured at this time is termed F_m. Under ambient light, the fluorescence is termed steady-state fluorescence (F_s). With this understanding, the following equations can be utilized (Baker 2008):

$$\Phi\text{PSII} = (F'_m - F_s)/F'_m. \quad (3)$$

The value represents the efficiency of PSII, or the proportion of photons utilized for electron transport. The equation below estimates non-photochemical quenching yield, or the proportion of photons used in non-photochemical quenching. By using values from dark-adapted fluorescence measurements, and the daily survey type PAM measurements, ΦNPQ could be calculated with the following equation:

$$\Phi\text{NPQ} = \frac{F}{F'_m} - \frac{F}{F_m}. \quad (4)$$

Eqs. 1, 3, and 4 can be used to estimate ΦF + ΦD, by substituting ΦNPQ and ΦPSII for ΦNPQ and ΦP, respectively, into Eq. 1. A third value that can be derived from fluorescence analysis is electron transport rate, which was calculated through the following equation (see *Data analysis* for the calculation of APAR):

$$\text{ETR} = \text{APAR} \times 0.5 \times \frac{F'_m - F_s}{F'_m}. \quad (5)$$

Here, 0.5 is used, assuming that one-half of absorbed photons go to PSII and the rest to PSI (Murchie and Lawson 2013).

Solar-induced chlorophyll fluorescence (SIF)

Passive fluorescence measurements were made by a portable spectrometer (QEpro, OceanOptics) that measures solar-induced fluorescence at the leaf-level. The portable spectrometer, covering the wavelength range between 670 and 780 nm, was connected to a bare fiber (1,000 μm, low-OH, sensitive for the visible and near-infrared region). We limited our analysis to the 730–780 nm region and retrieved SIF at 760 nm. The integrating time was set according the incident light intensity and the integration time was adjusted so the digital number (DN) at 755 nm was approximately around 100,000 each time. Generally, the integration time was around 50–200 ms, depending on the light intensity. A typical sequence of spectra collection initiated with measurement of a white spectralon panel (Labsphere, Hanover, New Hampshire, USA), then measuring the leaf at the nadir while keeping the leaf flat, and last collecting another spectrum from the white reference panel for a total of three measurements for each leaf. Dark currents were measured by closing the internal shutter of QEpro while keeping the integration time the same as during the measurement. The entire sequence took ~5 s for each leaf. The two white reference measurements were used to exclude any measurement where the light condition changed drastically. During the measurements, the detector was kept at −10°C to reduce noise and keep the signal-to-noise ratio high (nominal 1,000:1).

The portable spectrometer was calibrated with an integrating sphere in the lab (HELIOS, 246 Labsphere, North Sutton, New Hampshire, USA) during which a calibration file was generated containing the 247 calibration factor for the spectrometer. The HELIOS integrating sphere has a NIST-traceable lamp that was used for radiometric calibration. To product radiance spectra from the raw data, first, nonlinearity correction was conducted using coefficients provided by the manufacturer. Then the calibration file was used to convert the field measurements (in raw DN) to radiance ($\text{mw}\cdot\text{m}^{-2}\cdot\text{nm}^{-1}\cdot\text{sr}^{-1}$) and irradiance (by multiplying the panel radiance by π, giving $\text{mw}\cdot\text{m}^{-2}\cdot\text{nm}^{-1}$; Appendix S1: Fig. S1). The spectral fitting method was used to retrieve SIF at 760 nm (Meroni et al. 2009; see *Data analysis*). We calculated SIF_y, relative SIF yield, as the ratio between SIF at 760 nm and leaf radiance at 755 nm (Magney et al. 2019).

Data analysis

SIF was estimated using the spectral fitting method (SFM) with the irradiance (from the reference panel) and the leaf radiance (Meroni et al. 2009). The fraction of absorbed PAR (fAPAR) was calculated with the PROSPECT-D model (Féret et al. 2017) by using the measured chlorophyll concentration from SPAD-502 and assuming the carotenoid concentration was one-fifth the chlorophyll concentration. We then used PAR

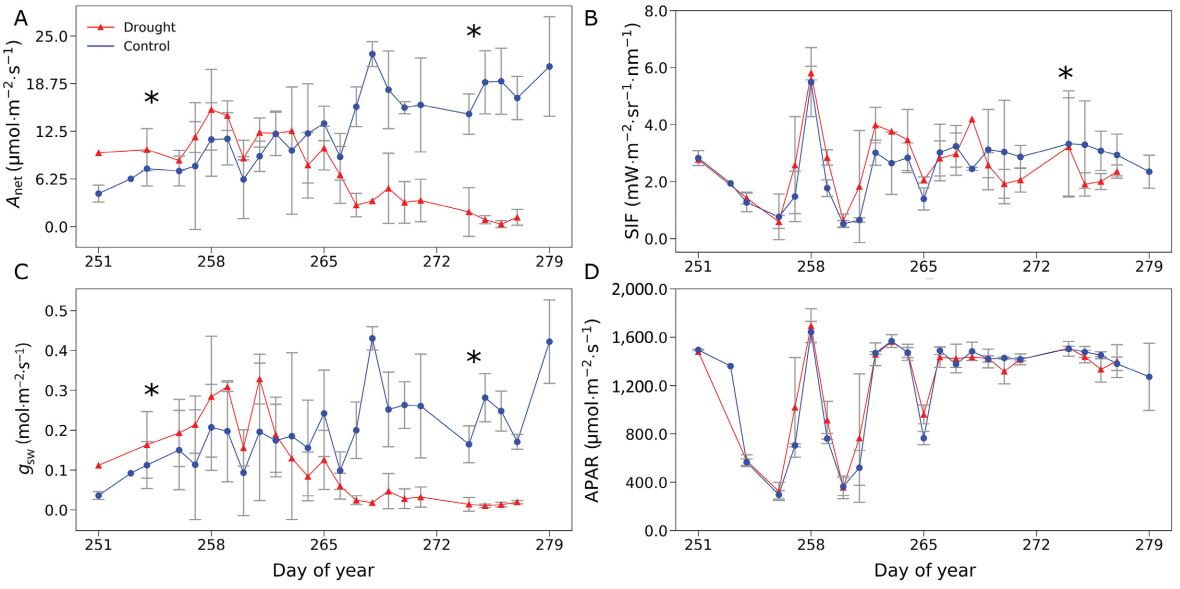

FIG. 1. Direct measurements of gas exchange and fluorescence during the drought experiment. Control individuals are in blue, and drought individuals are in red. (A) Average net photosynthesis of each treatment over the duration of the drought. (B) Average solar-induced chlorophyll fluorescence (SIF) of each treatment over the duration of the drought. (C) Average stomatal conductance of each treatment over the duration of the drought. (D) Average absorbed photosynthetically active radiation (APAR) over the duration of the drought. Note that the drought treatment began on day of year 251 (1 January = 1). Error bars represent standard deviation. Asterisks indicate statistically significant differences between drought and control treatments during first and/or last 10 d of experiment (*t* test, $\alpha = 0.05$; for the beginning of experiment, $n_{drought} = 19$, $n_{control} = 20$; for the end of the experiment, $n_{drought} = 18$, $n_{control} = 23$).

measured by the LI-6800 and fAPAR to estimate APAR, which was then used to calculate electron transport rate (Eq. 4).

RESULTS

A strong drought response was observed in gas exchange (Fig. 1A, C). The drought experiment started on the DOY 251, with water withheld from four plants and the other four maintained at field capacity. Both net photosynthesis (Fig. 1A) and stomatal conductance (Fig. 1C) decreased markedly 2 weeks into the drought (starting around DOY 265). By the third of week of the drought, both A_{net} and g_{sw} went down to near-zero in the drought plants while the control plants were photosynthesizing at a higher rate (18 μmol·m^{-2}·s^{-1}) than in the beginning of the experiment (on average 7.5 μmol·m^{-2}·s^{-1}). SIF shows a statistically significant difference between the drought plants and the control plants at the end of the experiment, although the response is much smaller than the change in gas exchange (Fig. 1B). During the entire period of experiment, there were no significant differences in APAR between the control and drought plants (Fig. 1D). The temporal variations in APAR result primarily from the day-to-day variation in light conditions.

SIF does not show as strong a drought response as the light reactions (Fig. 2 and Supplementary Figures for more analyses of the SIF–photosynthesis relationship). However, when normalized by steady-state fluorescence of dark-adapted leaves (F_o), a small drought response (i.e., drought individuals are statistically significantly lower than control individuals) is present in F_s/F_o, SIF/F_o, and SIF$_y$/F_o.

Steady-state fluorescence (F_s) in the NIR (beyond 710 nm) measured with the PAM-2500 is significantly correlated with relative SIF yield at 760 nm in both the drought plants and the control plants ($P < 0.01$). The control and the drought plants showed a similar relationship (Fig. 3A) and the two slopes are not significantly different; ANCOVA analysis returned a *P* value of 0.925. We also compared SIF$_y$ and ΦF + ΦD as given by Eq. 1. We found that SIF$_y$ is correlated with ΦD + ΦF, the residual of absorbed PAR after photochemistry and heat dissipation, suggesting that either ΦD and ΦF covary or ΦF dominates the variations in ΦD + ΦF. When calculated in this manner, we observe a close correlation between PAM-based ΦD + ΦF and SIF$_y$. Although this is expected from theory, here we see a correlation between fluorescence metrics measured with two different instruments despite PAM fluorescence being measured at a broader wavelength (>710 nm) than SIF (760 nm).

The ETR of drought plants shows a significant decline during the third week, but the magnitude of the decline is much less than that shown by A_{net} or g_{sw} (Fig. 4A).

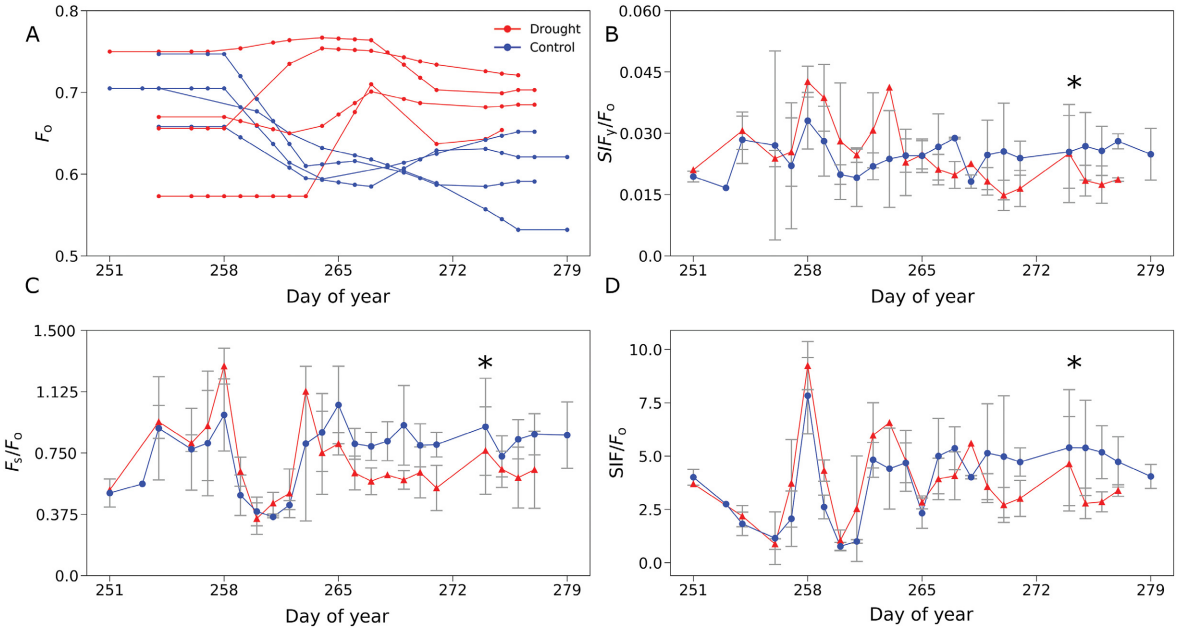

FIG. 2. (A) Minimal steady-state fluorescence in dark-adapted conditions. Each line represents a single plant. Days when dark-adapted measurements were not taken are interpolated. (B) When normalized for dark-adapted fluorescence (F_o), relative SIF yield shows a slight drought response. (C) Steady-state fluorescence (F_s) shows a drought response when normalized for F_o. (D) SIF shows a slight drought response when normalized for F_o. All points represent averages for each day, error bars represent standard deviations. Asterisks indicate statistically significant differences between drought and control treatments during first and/or last 10 d of experiment (t test, $\alpha = 0.05$; for the beginning of experiment, $n_{drought} = 19$, $n_{control} = 20$; for the end of the experiment, $n_{drought} = 18$, $n_{control} = 23$). Statistical tests were not conducted for F_o, as the data are interpolated.

There is a significant relationship ($R^2 = 0.468$ and 0.410, $P < 0.01$) between net carbon exchange and electron transport rate in both the control plants and the drought plants at the beginning of the experiment (Fig. 4B). As the drought continues, however, this relationship changes as gas exchange of the drought plants approaches zero while electron transport continues, although ETR decreases by almost two-thirds (black triangles in Fig. 4B).

The PAM fluorescence data on maximal light-adapted fluorescence (F'_m) show a clear effect of the drought treatment by DOY 265 (Fig. 5A), at the same time when the impact on gas exchange becomes apparent. Concurrently, there is an increase in non-photochemical quenching (and decrease of photochemical quenching) of the drought plants relative to the control (Fig. 5B).

It should be noted that the equation for ΦNPQ (Eq. 4) mixes measurements taken with different geometries of the fiber in relation to the leaf, which will affect the accuracy of the calculation. However, as shown below, we see ΦP + ΦNPQ is close to 0.9, as would be expected. Since ΦP is calculated without dark-adapted measurements, the room for error in this NPQ measurement is relatively small. Additionally, the high correlation with ΦP and ΦNPQ supports the idea that the uncertainty in NPQ is likely linear across leaves, and thus does not affect the overall pattern.

Across all plants in the experiment, drought plants and control plants, fluorescence and NPQ have strong inverse relationship when fluorescence values are normalized by F_o (Fig. 6A, B). Additionally, the data show a positive relationship between fluorescence and photosynthesis, although this relationship is weaker (Fig. 6C, D). Again, passively and actively measured fluorescence show a correlation (Fig. 6E).

DISCUSSION

Carbon cycling and gas exchange

As the use of SIF to estimate GPP increases (Yoshida et al. 2015, Zhang et al. 2018), it is important to understand how SIF relates to photosynthesis mechanistically, especially under stressful environmental conditions. If the relationship changes, the use of SIF to estimate GPP or to estimate drought may need careful consideration. We observe a strong stomatal response to drought stress, as evidenced by decreases in net photosynthetic carbon assimilation and stomatal conductance, while SIF shows a weaker drought response (Figs. 1, 2). Despite the correlation between GPP and SIF observed at global, regional, and ecosystem scales (Meroni et al. 2009, Yang et al. 2015, Sun et al. 2017, Li et al. 2018, Miao et al. 2018, Ryu et al. 2019), as well as leaf-level fluorescence

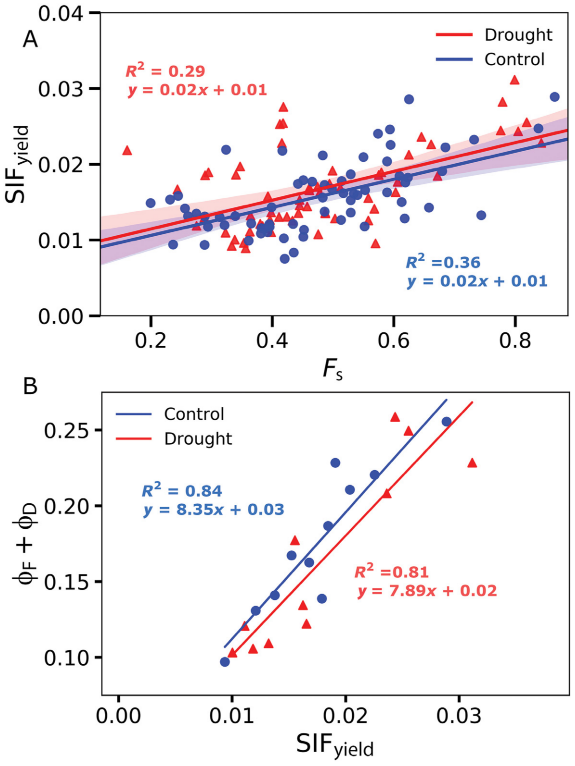

FIG. 3. (A) The correlation between relative SIF yield at 760 nm and steady-state fluorescence (F_s) measured by pulse amplitude modulated (PAM) fluorescence under drought (red triangles) and control (blue dots) conditions. The relationship is not significantly different between both the drought plants and the control plants. Shaded areas represent 95% confidence intervals. (B) Calculations from PAM fluorescence of the proportion of energy dissipating as fluorescence and basal heat dissipation also correlate with SIF yield.

and photosynthesis relationships under unstressed and stressed conditions (Flexas et al. 2002), the results here demonstrate that SIF does not show as large a response to drought stress as both net carbon exchange and stomatal conductance do, at least at the time scale of this drought experiment (weeks to a month). These data indicate that there are several complicating factors affecting the leaf-level SIF response to drought.

As often used by the eddy covariance community and in many SIF-GPP studies, GPP is defined as the difference between gross photosynthesis and photorespiration, while net photosynthesis as measured from a leaf-level gas exchange system (e.g., LI-6800) is intended to be the difference between gross photosynthesis, dark respiration, and photorespiration. Thus we have GPP = (gross photosynthesis) − photorespiration and A_{net} = (gross photosynthesis) − (dark respiration) − (photorespiration) (see Wohlfahrt and Gu 2015).

Conceptually then, GPP = A_{net} + (dark respiration). From a leaf-level mechanistic perspective, for SIF to be an indicator of GPP, SIF should relate to the photochemistry in the light reactions of photosynthesis, which relates to electron transport, which relates to carbon assimilation (This logical chain of relationships can be seen in Appendix S1: Fig. S10). At the leaf level, the response of the light reactions may be muted compared to the stomatal response, as increases in NPQ and the proportion of open PSII reaction centers compensate for decreases in photochemistry, dampening the impact on SIF (Schlau-Cohen and Berry 2015, Gu et al. 2019). Differences in the timing and magnitude of drought response are shown in the table below.

As shown in both Fig. 1 and Table 1, the stomatal response occurs earlier, and at a larger magnitude, than the fluorescence response. We suggest several potential processes that may change these relationships during drought stress: increasing photorespiration, upregulation of NPQ, and changes in internal leaf structure and/or chlorophyll content.

Research on drought stress in C_3 plants suggests that drought has several affects, with the first being stomatal closure. This causes a decrease in internal CO2 concentration, leading to an increase in photorespiration (which serves as an energy dissipation mechanism). During moderate drought stress, heat dissipation in the form of NPQ is upregulated, and under severe drought sustained forms of NPQ can lead to photoinhibition or damage of PSII reaction centers (Flexas and Medrano 2002, Medrano 2002). These factors could affect the relationship between SIF and photosynthesis. Using our data, with corroborating evidence from the literature, we suggest how the presence of these factors may affect the SIF–photosynthesis relationship.

There is a correlation between the electron transport rate (ETR) and net photosynthesis among the control plants and the early stage drought plants (Fig. 4B), indicating a coordination between the light reactions and carbon fixation. During drought, the relationship decouples, as the drought plants continued to have electron transport despite no net photosynthesis (Figs. 1, 4). This is likely due to an increase in photorespiration induced by drought stress, altering the relationship between net photosynthetic carbon exchange and the light reaction aspects of photosynthesis (Flexas et al. 1999, 2000, 2002). Alteration of this relationship decouples SIF and photosynthesis during environmental stress. The response of the light reactions and dark reactions of photosynthesis may operate on different time scales altering the relationship (Gu et al. 2019).

Further insight into the relationship between SIF and photosynthetic products is provided by the pulse amplitude modulated fluorescence analysis. Steady-state fluorescence (F_s) and SIF$_y$ are tightly correlated (Fig. 3), as has been shown at the leaf scale when averaging multiple leaves (Cendrero-Mateo et al. 2016). This result confirms that SIF measured at one single wavelength (760 nm) agrees with the broadband (>710 nm) passive fluorescence that PAM measured.

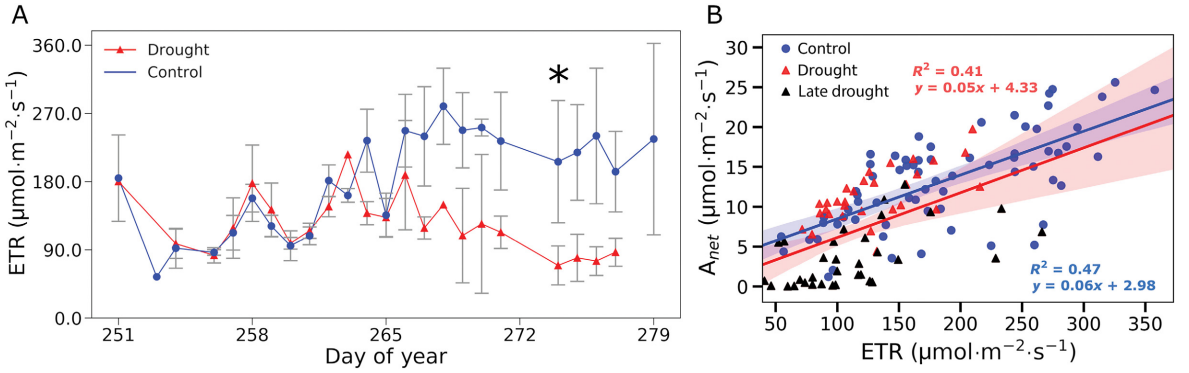

FIG. 4. (A) Average electron transport rate (ETR) for each treatment during the drought. The drought plants show decreases in electron transport rate during the drought. Error bars represent standard deviations. (B) Net photosynthesis and electron transport rate were found to have a strong relationship. The relationship is the same for both the control plants and the drought plants before the drought. The black triangles represent points not included in the regression analysis, they indicate values for the last 15 d of the drought when A_{net} and stomatal conductance were both close to zero. Shaded areas represent 95% confidence intervals. Asterisks indicate statistically significant differences ($P \leq 0.05$) between drought and control treatments during first and/or last 10 d of experiment (t test, $\alpha = 0.05$; for the beginning of experiment, $n_{drought} = 19$, $n_{control} = 20$; for the end of the experiment, $n_{drought} = 18$, $n_{control} = 23$).

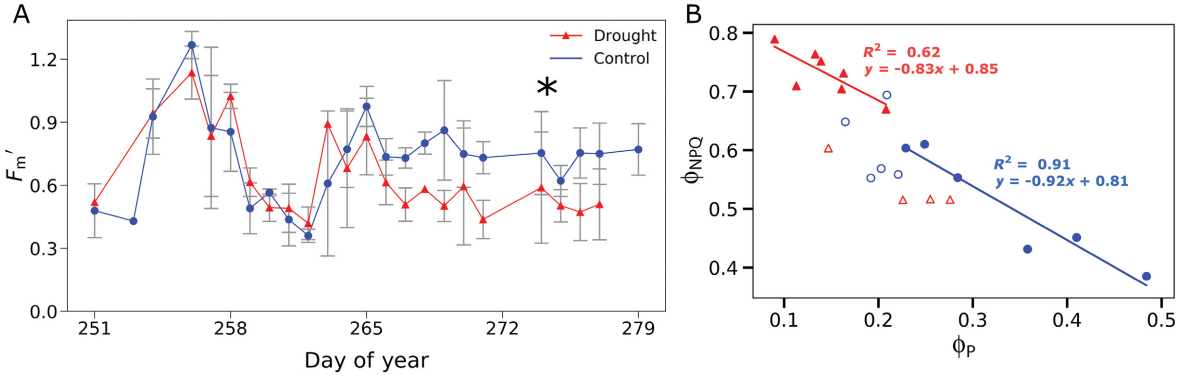

FIG. 5. (A) Average maximum light-adapted fluorescence decreased in the drought plants relative to the control. Error bars represent standard deviation. (B) Energy partitioning to non-photochemical quenching (NPQ) and photochemistry. The hollow points are before drought effects (day of year < 265). Portioning of energy to NPQ in the drought plants increased relative to the control. Asterisks indicate statistically significant differences ($P \leq 0.05$) between drought and control treatments during first and/or last 10 d of experiment (t test, $\alpha = 0.05$; for the beginning of experiment, $n_{drought} = 19$, $n_{control} = 20$; for the end of the experiment, $n_{drought} = 18$, $n_{control} = 23$).

The drought plants showed a clear decrease in F'_m (Fig. 5A) corresponding to an increase in NPQ (Fig. 5B). Drought stress leading to an upregulation of NPQ is a relatively well-established phenomenon, and has been suggested to lead to a decoupling of SIF from photosynthetic carbon assimilation under stress (Porcar-Castell et al. 2014, Cendrero-Mateo et al. 2015, Wohlfahrt et al. 2018, Xu et al. 2018). The smaller response of SIF to drought stress, when compared to PQ and NPQ may be due to complementarity between PQ and NPQ. Under drought stress, the decrease in PQ may be compensated by an increase in NPQ, affecting fluorescence relatively little, despite large changes in PQ. Although NPQ and fluorescence are negatively correlated, the complementarity between PQ and NPQ likely dominates this trade-off (Fig. 6, Appendix S1: Fig. S5).

Additionally, the drought plants show a slight decrease in the maximum efficiency of PSII, F_v/F_m, (where F_v equals $F_m - F_o$, see Appendix S1: Fig. S6), an indication that the plant is experiencing photoinhibition, which has been shown to occur under severe drought stress (Krause and Weis 1991, Adams and Demmig-Adams 2004, Murchie and Lawson 2013, Porcar-Castell et al. 2014). Lowered F_v/F_m after in dark-adapted leaves could also be indicative of sustained upregulation NPQ. Although depressed F_v/F_m is not seen in some studies of drought stress (Flexas et al. 1998), it has been suggested as a stress-coping mechanism in other species (Adams and Demmig-Adams 2004). Interspecific variation in drought stress response is beyond the scope of this study, but different stress responses (stomatal vs. photochemical) could lead to different chlorophyll fluorescence responses to drought.

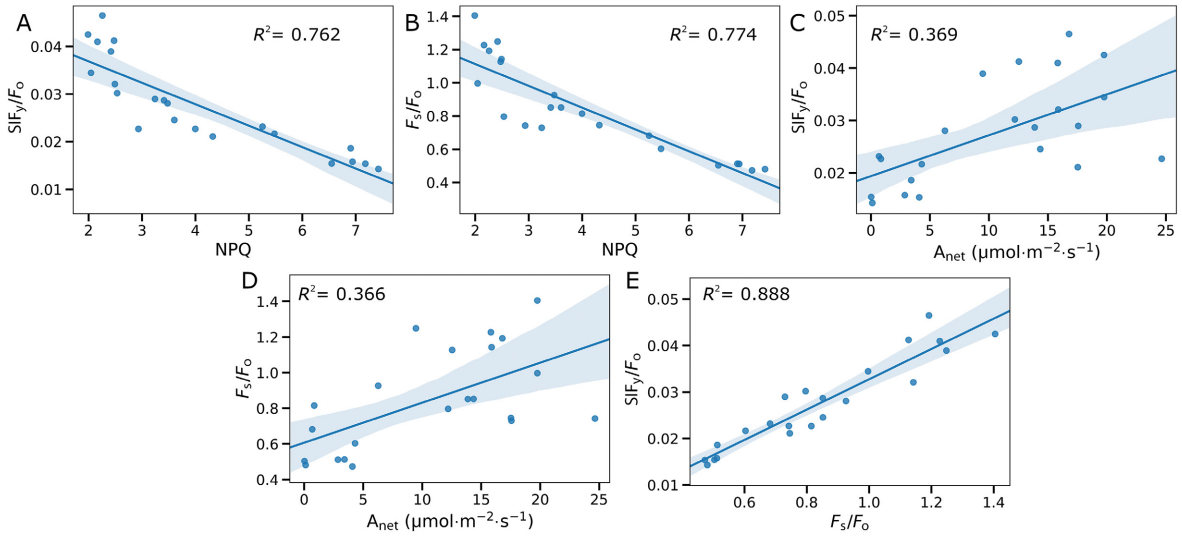

FIG. 6. Normalized relationships among key fluorescence parameters on days where dark-adapted measurements were taken to obtain F_o. Fluorescence and NPQ have a strong negative relationship (A and B). Both passive and active fluorescence show weak positive relationships with gas exchange (C and D). Passively and actively measured fluorescence are correlated (E). All values, drought and control, are included in the plots.

TABLE 1. Timing of responses and difference between drought and control at the end of the experiment.

Parameter	Response timing (DOY)	Relative difference (last 5 d)
Net assimilation	263–267	0.958
Stomatal conductance	263–267	0.95
SIF	275–279	0.321
F_s/F_o	273–277	0.22
SIF_y	275–279	0.214

Notes: Timing of response was found by conducting two-sample *t*-tests along a 5-d moving window. The time period shown in the table is when the difference between drought and control was statistically significant ($\alpha = 0.05$) for the rest of the experiment. The relative difference was calculated over the last 5 d of the experiment as the difference in means between drought and control divided by control. DOY, day of year, with 1 January = 1; SIF, solar-induced chlorophyll fluorescence; F_o, dark-adapted fluorescence; F_s, steady-state fluorescence.

These fluorescence data suggest another possible explanation for the SIF/gas exchange disjunction. Similar to canopy structural changes during drought (i.e., changes in leaf area or leaf angles, see Kao and Forseth 1992), rearrangements of chlorophyll molecules within the cell, or changing chlorophyll concentration, can affect leaf optical properties and change the net SIF emitted from a leaf (Vilfan et al. 2016). The SIF measured from a leaf (or a canopy) is the difference between the total amount of fluorescence emitted and the amount of fluorescence absorbed within the leaf (or, in the case of canopies, by other leaves). Minimal dark-adapted fluorescence (F_o) increased in the drought plants (Fig. 3a), which can be an indication of drought affecting leaf optical properties (Baker 2008, Murchie and Lawson 2013). If drought induces cellular reorientation or chlorophyll concentration changes, then the proportion of SIF reabsorbed could decline, dampening the observed decline in emitted SIF. The absorbance and chlorophyll concentration decreased during the experiment in the drought plants, congruent with the idea that leaf optical properties changed during the drought (see Appendix S1: Fig. S3).

Limitations of this study

The limitations of this study should also be addressed. The PAM measurements taken in light conditions and dark-conditions are at different fiber orientations, adding error in these measurements. Additionally, the dark-adapted measurements are not taken every day, instead we interpolated between measurements with the assumption that F_m and F_o do not change as fast as F_s, which may introduce some uncertainty. Lastly, our measurements are taken sequentially not simultaneously, preventing direct, instantaneous comparison of measurements. We show in the results that there are correlations between measurements taken with different instruments, suggesting that this limitation, although introducing error, does not prevent comparison. Improving these limitations, along with testing postulations mentioned in the discussion, provide exciting directions for future SIF studies.

Implications

This study demonstrates the importance and necessity for a physiological understanding of SIF. These results

suggest that using SIF across a broad range of environmental conditions may be nontrivial, especially in the case of drought. As demonstrated, SIF does not provide a direct estimate of the carbon cycling component of photosynthesis on the leaf scale under the short drought conditions of this experiment. There are several complicating factors impacting the leaf-level response of SIF to drought.

As shown in Fig. 2, there is a slight observed decrease in both normalized SIF and F_s/F_o in the plants under drought stress. The correlation is likely due to changes in photosynthetic regulation that, in certain circumstances, cause a correlated decrease in both photosynthesis and fluorescence. Interestingly, in the study by Flexas et al. (2002), PPFD is lower than our normal APAR. At extremely high light values, Flexas et al. (2002) see F_s decline, even in well-watered plants (Flexas et al. 2002). The high ambient light intensity outdoors could also be a potential explanation for a dampened fluorescence response. Further research in controlled environments is needed to elucidate the mechanisms behind the SIF drought response. Care should be taken when performing SIF studies to ensure appropriate use of the measurement. When using SIF as a proxy for drought stress these potential complications should be considered. As we can see that the SIF response to water stress is much smaller than that of gas exchange, thus it requires highly accurate measurements of SIF to ensure a detectable response.

Another noteworthy observation is the correlation between SIF relative yield and steady-state PAM fluorescence (F_s). This is to be expected as both passively measure leaf fluorescence, but demonstrating a relationship has further implications. PAM fluorescence is an established measurement technique with a solid mechanistic basis. This linkage could provide opportunities for improving our understanding of SIF mechanisms. In addition, the tight relationship between SIF measured at a single wavelength (760 nm) and the broadband (710 nm and beyond) PAM fluorescence indicate that the variability of the shape of fluorescence in the NIR region is likely small (Magney et al. 2017).

The effect of short-term drought on the relationship between SIF and gas exchange at the single leaf scale offers exciting insights into the mechanisms underlying SIF variability. The results also raise interesting cautionary flags involving the use and interpretation of SIF to estimate productivity across environmental conditions. It is possible that changes at the whole-plant and canopy scales ameliorate (or, perhaps, amplify) what has been found at the scale of single leaf held at a fixed angle. At the canopy scale, the response is not the sum of individual leaves, but rather a product of the canopy structure, which is also changing. The drought response of SIF detectable by satellites could be a combination of canopy structure, and single leaf physiology, with the former potentially a stronger control. Future efforts to investigate the SIF-gas exchange relationship should examine these higher organizational scales and consider how other biological factors, e.g., canopy structure, might also modulate the relationships. As mechanistic understanding increases it will be possible to move beyond empirical correlations when using SIF to estimate ecosystem processes.

Acknowledgments

We thank the following people for assistance with this research, Wenzheng (Andie) Wang and Wendy Crannage. We also thank the anonymous reviewers of this manuscript; their comments on earlier versions were very helpful. X. Yang was partly supported by the NASA Interdisciplinary Science (IDS) program (80NSSC17K0110) and US-NSF Atmospheric Chemistry Program (1837891). M. T. Lerdau acknowledges the support of the US-NSF Atmospheric Chemistry Program (1837891). L. Helm, M. T. Lerdau, and X. Yang designed the experiment. L. Helm, X. Yang, and H. Shi conducted the experiment. L. Helm, M. T. Lerdau, and X. Yang wrote the paper.

Literature Cited

Adams, W. W., and B. Demmig-Adams. 2004. Chlorophyll fluorescence as a tool to monitor plant response to the environment. Pages 583–604 *in* G. C. Papageorgiou, and Govindjee, editors. Chlorophyll a fluorescence: a signature of photosynthesis. Springer, Berlin, Germany.

Baker, N. R. 2008. Chlorophyll fluorescence: a probe of photosynthesis in vivo. Annual Review of Plant Biology 59:89–113.

Beer, C., et al. 2010. Terrestrial gross carbon dioxide uptake: global distribution and covariation with climate. Science 329:834–838.

Berry, J. A., C. Frankenberg, and P. Wennberg. 2013. New Methods for measurement of photosynthesis from space. Keck Institute for Space Studies, Pasadena, California, USA.

Cendrero-Mateo, M. P., A. E. Carmo-Silva, A. Porcar-Castell, E. P. Hamerlynck, S. A. Papuga, and M. S. Moran. 2015. Dynamic response of plant chlorophyll fluorescence to light, water and nutrient availability. Functional Plant Biology 42:746–757.

Cendrero-Mateo, M. P., M. S. Moran, S. A. Papuga, K. R. Thorp, L. Alonso, J. Moreno, G. Ponce-Campos, U. Rascher, and G. Wang. 2016. Plant chlorophyll fluorescence: active and passive measurements at canopy and leaf scales with different nitrogen treatments. Journal of Experimental Botany 67:275–286.

Demmig-Adams, B., and W. W. Adams. 2006. Photoprotection in an ecological context: the remarkable complexity of thermal energy dissipation. New Phytologist 172:11–21.

Féret, J. B., A. A. Gitelson, S. D. Noble, and S. Jacquemoud. 2017. PROSPECT-D: towards modeling leaf optical properties through a complete lifecycle. Remote Sensing of Environment 193:204–215.

Flexas, J., and H. Medrano. 2002. Energy dissipation in C3 plants under drought. Functional Plant Biology 29:1209–1215.

Flexas, J., J. M. Escalona, and H. Medrano. 1998. Down-regulation of photosynthesis by drought under field conditions in grapevine leaves. Functional Plant Biology 25:893–900.

Flexas, J., J. M. Escalona, and H. Medrano. 1999. Water stress induces different levels of photosynthesis and electron transport rate regulation in grapevines. Plant, Cell & Environment 22:39–48.

Flexas, J., J.-M. Briantais, Z. Cerovic, H. Medrano, and I. Moya. 2000. Steady-state and maximum chlorophyll

fluorescence responses to water stress in grapevine leaves: a new remote sensing system. Remote Sensing of Environment 73:283–297.

Flexas, J., J. M. Escalona, S. Evain, J. Gulias, I. Moya, C. B. Osmond, and H. Medrano. 2002. Steady-state chlorophyll fluorescence (Fs) measurements as a tool to follow variations of net CO2 assimilation and stomatal conductance during water-stress in C3 plants. Physiologia Plantarum 114:231–240.

Frankenberg, C., et al. 2011. New global observations of the terrestrial carbon cycle from GOSAT: Patterns of plant fluorescence with gross primary productivity. Geophysical Research Letters 38: L17706.

Funk, J. L., C. G. Jones, and M. T. Lerdau. 1999. Defoliation effects on isoprene emission from *Populus deltoides*. Oecologia 118:333–339.

Funk, J. L., J. E. Mak, and M. Lerdau. 2004. Stress-induced changes in carbon sources for isoprene production in *Populus deltoides*. Plant, Cell and Environment 27:747–755.

Funk, J., C. Jones, and M. Lerdau. 2007. Leaf- and shoot-level plasticity in response to varying nutrient and water availability in *Populus deltoides*. Tree Physiology. 27:1731–1739.

Genty, B., J. M. Briantais, and N. R. Baker. 1989. The relationship between the quantum yield of photosynthetic electron transport and quenching of chlorophyll fluorescence. Biochimica et Biophysica Acta—General Subjects 990:87–92.

Gu, L., J. Han, J. D. Wood, C. Y.-Y. Chang, and Y. Sun. 2019. Sun-induced Chl fluorescence and its importance for biophysical modeling of photosynthesis based on light reactions. New Phytologist 223:1179–1191.

Heinz Walz GmbH. 2008. Portable chlorophyll fluorometer PAM-2500: handbook of operation. Heinz Walz GmbH, Effeltrich, Germany.

Isebrands, J. G., and P. R. Larson. 1973. Anatomical changes during leaf ontogeny in *Populus deltoides*. American Journal of Botany 60:199–208.

Joiner, J., Y. Yoshida, A. P. Vasilkov, Y. Yoshida, L. A. Corp, and E. M. Middleton. 2011. First observations of global and seasonal terrestrial chlorophyll fluorescence from space. Biogeosciences 8:637–651.

Kao, W.-Y., and I. N. Forseth. 1992. Diurnal leaf movement, chlorophyll fluorescence and carbon assimilation in soybean grown under different nitrogen and water availabilities. Plant, Cell & Environment 15:703–710.

Krause, G. H., and E. Weis. 1991. Chlorophyll fluorescence and photosynthesis: the basics. Annual Review of Plant Physiology and Plant Molecular Biology 42:313–349.

Lee, J.-E., J. A. Berry, C. van der Tol, X. Yang, L. Guanter, A. Damm, I. Baker, and C. Frankenberg. 2015. Simulations of chlorophyll fluorescence incorporated into the Community Land Model version 4. Global Change Biology 21:3469–3477.

Li, X., J. Xiao, and B. He. 2018. Chlorophyll fluorescence observed by OCO-2 is strongly related to gross primary productivity estimated from flux towers in temperate forests. Remote Sensing of Environment 204:659–671.

Magney, T. S., C. Frankenberg, J. B. Fisher, Y. Sun, G. B. North, T. S. Davis, A. Kornfeld, and K. Siebke. 2017. Connecting active to passive fluorescence with photosynthesis: a method for evaluating remote sensing measurements of Chl fluorescence. New Phytologist 215:1594–1608.

Magney, T. S., et al. 2019. Mechanistic evidence for tracking the seasonality of photosynthesis with solar-induced fluorescence. Proceedings of the National Academy of Sciences USA 116:11640–11645.

Medrano, H. 2002. Regulation of photosynthesis of C3 plants in response to progressive drought: stomatal conductance as a reference parameter. Annals of Botany 89:895–905.

Meroni, M., M. Rossini, L. Guanter, L. Alonso, U. Rascher, R. Colombo, and J. Moreno. 2009. Remote sensing of solar-induced chlorophyll fluorescence: review of methods and applications. Remote Sensing of Environment 113:2037–2051.

Miao, G., et al. 2018. Sun-induced chlorophyll fluorescence, photosynthesis, and light use efficiency of a soybean field from seasonally continuous measurements. Journal of Geophysical Research: Biogeosciences 123:610–623.

Mohammed, G. H., et al. 2019. Remote sensing of solar-induced chlorophyll fluorescence (SIF) in vegetation: 50 years of progress. Remote Sensing of Environment 231:111177.

Murchie, E. H., and T. Lawson. 2013. Chlorophyll fluorescence analysis: a guide to good practice and understanding some new applications. Journal of Experimental Botany 64:3983–3998.

Parazoo, N. C., K. Bowman, J. B. Fisher, C. Frankenberg, D. B. A. Jones, A. Cescatti, Ó. Pérez-Priego, G. Wohlfahrt, and L. Montagnani. 2014. Terrestrial gross primary production inferred from satellite fluorescence and vegetation models. Global Change Biology 20:3103–3121.

Porcar-Castell, A., E. Tyystjärvi, J. Atherton, C. Van Der Tol, J. Flexas, E. E. Pfündel, J. Moreno, C. Frankenberg, and J. A. Berry. 2014. Linking chlorophyll a fluorescence to photosynthesis for remote sensing applications: Mechanisms and challenges. Journal of Experimental Botany 65:4065–4095.

Raczka, B., et al. 2019. Sustained nonphotochemical quenching shapes the seasonal pattern of solar-induced fluorescence at a high-elevation evergreen forest. Journal of Geophysical Research: Biogeosciences 124:2005–2020.

Ryu, Y., J. A. Berry, and D. D. Baldocchi. 2019. What is global photosynthesis? History, uncertainties and opportunities. Remote Sensing of Environment 223:95–114.

Schaefer, K., et al. 2012. A model-data comparison of gross primary productivity: results from the North American carbon program site synthesis. Journal of Geophysical Research Biogeosciences 117:G03010.

Schlau-Cohen, G. S., and J. Berry. 2015. Photosynthetic fluorescence, from molecule to planet. Physics Today 68:66–67.

Sun, Y., et al. 2017. OCO-2 advances photosynthesis observation from space via solar-induced chlorophyll fluorescence. Science 358:eaam5747.

van der Tol, C., J. A. Berry, P. K. E. Campbell, and U. Rascher. 2014. Models of fluorescence and photosynthesis for interpreting measurements of solar-induced chlorophyll fluorescence. Journal of Geophysical Research: Biogeosciences 119:2312–2327.

Verma, M., et al. 2014. Remote sensing of annual terrestrial gross primary productivity from MODIS: an assessment using the FLUXNET La Thuile data set. Biogeosciences 11:2185–2200.

Vilfan, N., C. van der Tol, O. Muller, U. Rascher, and W. Verhoef. 2016. Fluspect-B: a model for leaf fluorescence, reflectance and transmittance spectra. Remote Sensing of Environment 186:596–615.

Wohlfahrt, G., and L. Gu. 2015. The many meanings of gross photosynthesis and their implication for photosynthesis research from leaf to globe. Plant, Cell & Environment 38:2500–2507.

Wohlfahrt, G., K. Gerdel, M. Migliavacca, E. Rotenberg, F. Tatarinov, J. Müller, A. Hammerle, T. Julitta, F. M. Spielmann, and D. Yakir. 2018. Sun-induced fluorescence and gross primary productivity during a heat wave. Scientific Reports 8:14169.

Xu, S., Z. Liu, L. Zhao, H. Zhao, and S. Ren. 2018. Diurnal response of sun-induced fluorescence and PRI to water stress

in maize using a near-surface remote sensing platform. Remote Sensing 10:1510.

Yang, X., J. Tang, J. F. Mustard, J. E. Lee, M. Rossini, J. Joiner, J. W. Munger, A. Kornfeld, and A. D. Richardson. 2015. Solar-induced chlorophyll fluorescence that correlates with canopy photosynthesis on diurnal and seasonal scales in a temperate deciduous forest. Geophysical Research Letters 42:2977–2987.

Yang, H., X. Yang, Y. Zhang, M. A. Heskel, X. Lu, J. W. Munger, S. Sun, and J. Tang. 2017. Chlorophyll fluorescence tracks seasonal variations of photosynthesis from leaf to canopy in a temperate forest. Global Change Biology 23:2874–2886.

Yang, X., H. Shi, A. Stovall, K. Guan, G. Miao, Y. Zhang, Y. Zhang, X. Xiao, Y. Ryu, and J. E. Lee. 2018. FluoSpec 2—an automated field spectroscopy system to monitor canopy solar-induced fluorescence. Sensors 18:2063.

Yoshida, Y., J. Joiner, C. Tucker, J. Berry, J.-E. Lee, G. Walker, R. Reichle, R. Koster, A. Lyapustin, and Y. Wang. 2015. The 2010 Russian drought impact on satellite measurements of solar-induced chlorophyll fluorescence: Insights from modeling and comparisons with parameters derived from satellite reflectances. Remote Sensing of Environment 166:163–177.

Zhang, Y., J. Joiner, P. Gentine, and S. Zhou. 2018. Reduced solar-induced chlorophyll fluorescence from GOME-2 during Amazon drought caused by dataset artifacts. Global Change Biology 24:2229–2230.

Supporting Information

Additional supporting information may be found online at: http://onlinelibrary.wiley.com/doi/10.1002/eap.2101/full

Data Availability

Data are available on Figshare: https://doi.org/10.6084/m9.figshare.9968372.v1